13. **V.V. Lukinov, A.P. Klec, B.V. Bokij, I.A. Efremov**, Ugol' Ukrainy. **1**, 50-53 (2011)

14. **V.V. Bokij, O.I. Kasimov,** Ugol' Ukrainy. **5**, 17-21 (2005).

15. **Kryzhanovskij, Y., & Antoshchenko, N.** (2014). O maksimal'nom gazovydelenii v gornye vyrabotki pri otrabotke ugol'nyh plastov (R. Gasyuk, Ed.). Sb. Nauchnyh Trudov MakNII, 2(32), 69-76.

https://doi.org/10.31713/m1016

MODELING OF PHOSPHORUS PRODUCTION PROCESSES AND DEVELOPING A MANAGEMENT STRUCTURE BASED ON GREY SYSTEMS

Toktasynova Nigina
Satbayev University, Master of Engineering and Technology, Junior Researcher of Department “Automation and Control”, Kazakhstan

Suleimenov B. A.
Satbayev University, Doctor of Engineering Sciences, Professor of Department “Automation and Control”, Kazakhstan.
Hassen Fourati, PhD, Associate Professor of Gipsa Lab, Grenoble, France

Kulakova Ye.A.
Satbayev University, Master of Engineering and Technology, Lecturer of Department “Automation and Control”, Kazakhstan

Abstract

The agglomeration process is one of the complex, multidimensional technological processes; it takes place under conditions of a large number of disturbing influences. As a result, the amount of return during sintering reaches 40-50%.

The work is devoted to the development of a mathematical model capable of predicting and controlling the sintering point based on real-time data. As the main parameters for the construction of predictive models, data measured in real time were used – the temperature in the vacuum chambers and the gas velocity determined through the measured pressure (rarefaction) in the vacuum chambers.

This paper describes the methodology and basic algorithms for modeling agglomeration processes, starting from the ingress of the charge into the sinter machine and ending with the production of a suitable agglomerate. The obtained curves of the developed mathematical model of temperature in vacuum chambers served as the basis for testing the forecast model based on the use of the theory of gray systems and the optimization algorithm of the "swarm of particles". Based on the developed mathematical model, a system for predicting the sintering point is constructed, which is the basis for determining the quality of the agglomerate, which

will reduce the return volume during sintering. The general structure of the sinter control system based on a dynamic predictive model is also proposed.

The practical significance of the developed predictive model based on the theory of gray systems is as follows:

- forecast of the sintering point value of the agglomerate and synthesis of the control action based on the forecast;
- the algorithm for constructing a mathematical model of the forecast can be used for any process that has the character of a "gray exponential law".

Introduction

Agglomeration in metallurgy is a thermal process of sintering of a metallurgical charge consisting of granules of various metals and fuel. In terms of natural resources, agglomeration is a key technology for recycling products or dust from metallurgy. The raw materials used can vary widely from ore to recycled dust and fluxes.

The agglomeration process is a complex, multidimensional technological process; proceeds under conditions of a large number of disturbing influences: changes in the chemical-mineralogical, granulometric composition of the charge components; conditions of moistening, dosing, mixing and placing the charge on the surface of the sinter machine. The process is automated, but the control systems for the sintering process in modern production facilities do not allow ensuring the maximum productivity of sinter machines and the constancy of high quality of the output product.

Agglomeration is a nonlinear process, which makes real-time quality management of the final product challenging. In practice, the process is controlled with a delay: the operator changes the process parameters after receiving the final product, which leads to the appearance of a return, i.e. sinter, which must be returned to the initial stage for re-processing. The return can be up to 40-50% of the final sinter, which significantly increases the cost of the process, and also introduces uncertainty into the composition of the initial charge.

Improving the quality of the sinter can be achieved both by process change - optimizing the composition of the charge, the size of the granules, changing the amount of fuel, water, etc., and by process control - controlling the speed of pallet movement, discharge in vacuum chambers, and by the height of the charge.

The solution of the task of process change leads to the need to use an analytical modeling method that uses the

physicochemical 3 processes that occur during agglomeration. The advantage of the analytical method lies in the completeness of constructing a model that takes into account all the processes of agglomeration and allows research and experiments on the basis of the model. Moreover, this method is universal for modeling similar processes. The problem of using and adapting existing models for the process of agglomeration of phosphorite ores is that this process is not widespread, and the use of ready-made models for the agglomeration of iron ores is impossible due to the differences in the chemical reactions. This circumstance leads to the need to create an original model of sinter roasting of phosphorus-containing materials.

Modern methods for solving the task of process control are based on an empirical research method, which consists in collecting a large amount of data and in creation of a model based on training algorithms. This method involves performing experiments on an object to obtain a representative data sample. At the moment, models created on the basis of neural networks are increasingly used for technological processes. The disadvantage of this method is the need for a large amount of data and retraining the model when the process conditions change. This fact is critical for the agglomeration process, due to the change in the composition of the charge, which depends on both the mineralogical properties of the ore and the amount of return. In connection with the above mentioned, it becomes necessary to create a model using a small amount of information and allowing retraining the model in real time.

1 THE CURRENT STATE OF MATHEMATICAL MODELING OF THE AGLOMERATION PROCESS

1.1 Description of the agglomeration process

Agglomeration in metallurgy is a thermal process of sintering of fine materials that are constituent parts of a metallurgical charge. The agglomeration process is a complex nonlinear system with a large delay, in which many process parameters are interrelated, and the sintering process takes place with different chemical transformations

at each stage of the sinter machine operation and on different layers of the sinter.

The process of agglomeration of phosphorite ores is carried out at the Novodzhambul Phosphoric Plant (NDPP) [1], located in the south of Kazakhstan, near the Karatau deposit. Agglomeration method consists in sintering phosphorite fines on an AKM-7-312 sinter machine at temperatures up to 1623 K using crushed coke as a solid fuel. Agglomeration is the second most important process on the plant, after the production of yellow phosphorus, for which the sinter is the raw material. The technological process (Figure 1.1) begins with the initial mixing of the charge with cold and tertiary return, which is fed without dosing, which leads to significant changes in the fuel in the charge. Then the charge is sent to the moving belt, where it is ignited with natural gas or CO2, passing through the hearth. Sinter gases are sucked off through 26 vacuum chambers located under the sinter machine. Due to the vacuum created in the vacuum chambers, the heat from the combustion of the fuel gradually moves to the underlying layers, uniformly sintering a layer of 260 mm and goes to the end of the 78 m long belt. Temperature and vacuum control is provided in all vacuum chambers. The regulation of the vacuum in the vacuum chambers is carried out using dampers, which are remotely controlled from the control panel of the sinter machine. Then the sinter is cooled, crushed to the required size and, after sorting, is sent to the batching department of the furnace room No. 05, and the poor quality sinter is sent to the beginning of the process.

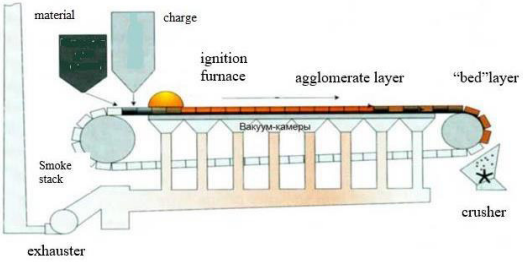

Fig. 1.1. Schematic representation of the sinter machine

1.2 Characteristic features of mathematical models of the agglomeration process

Let's highlight the main characteristic features of mathematical models of the agglomeration process:

1. Like any mathematical model, they are subdivided into one-dimensional, two-dimensional and three-dimensional in relation to the dimension of space (table 1.1).

2. During the sintering process, the charge undergoes three phase states: solid, gaseous and liquid.

3. The main mechanism of heat transfer considered during the sintering process is convection, which forms the basis of heat transfer during sintering.

4. The main equation of motion of the gas phase or the equation of moment is the Ergun equation for porous medium

$$\frac{\Delta p}{L} = \frac{150\mu u(1-\varepsilon)^2}{d^2\varepsilon^3} + \frac{1{,}75\rho u^2(1-\varepsilon)}{d\varepsilon^3},$$

where Δp - pressure drop, L - height charge, μ - viscosity, ε - porosity, ρ - density, d - granule diameter, u - air flow rate.

Table 1.1

Comparative analysis of various agglomeration models

Ref.	Objective	Type	Phase	Types of heat transfer	Combustion of coke	Chemical reactions	Gas flow equation	Condensation and Evaporation	Porosity	Result
[6]	Modeling structural changes in the sinter	1-D	Solid, gaseous	Convection	$C+O_2 \rightarrow CO_2$	Decomposition of $CaCO_3$	Unknown	Evaporation rate as a dependence from particle diameter	Changing the radius of particles due to combustion	Study of the effect of coke content and melting temperature on the sinter structure
[7]	Modeling the agglomeration process with a focus on the speed of the heat front through the layer	1-D	Solid, gaseous	Convection, Thermal conductivity	$(1+\varphi)C + \left(1+\frac{\varphi}{2}\right)O_2 \rightarrow \varphi CO + CO_2$, $CO + 1/2O_2 \rightarrow CO_2$	Decomposition of $CaCO_3$, $FeCO_3$, $MgCO_3$, $MnCO_3$. Arrhenius equation. Nonlinear regression equation for CaO and $Ca(OH)_2$	Modified Ergun Equation	Evaporation temperature equation depending on pressure	Through particle shrinkage model	The most sensitive process parameters are determined
[8]	Modeling of the process in a multilayer solid phase, taking into account porosity and shrinkage with geometric changes	1-D	Several solid, gaseous	Convection, thermal conductivity, radiation	$CO + 1/2O_2 \rightarrow CO_2$, $C + 1/2O_2 \rightarrow CO$	Decomposition of $CaCO_3$	Input air rate - function of time - 2nd order polynomial. Pressure drop not taken into account	Through reactions solid-gaseous phases	Geometric changes in the sinter associated with reactions between solid and gas	Analysis of the influence of 3 different coke contents on sinter temperature and gas composition
[14]	Model of changes in the structure of the sinter: pore ratio, mineralogical composition, quality of the sinter	3-D	Solid, gaseous, liquid	Convection, Thermal conductivity Rans-Marshall equation for heat transfer between 2 phases and Cooney-Smith equation - for thermal conductivity	$C+O_2 \rightarrow CO_2$	Decomposition of $CaCO_3$ $MgCO_3$, Fe_2CO_3	Ergun Equation	$H_2O(l) \Rightarrow H_2O(g)$	The change in porosity is represented by pseudo particles, which disappear after the equations of porosity, combustion and decarbonization	Consideration of changes in sinter quality and throughput by installing a gas flow tray
[9]	Determination of the optimal structure of the 2-level process – the hydrocarbon content at each level and determination of the layer thickness	2-D	Solid, gaseous,	Convection according to the Kuni-Suzuki equation	$C+O_2 \rightarrow CO_2$, $2C + O_2 \rightarrow 2CO$, $C+CO_2 \rightarrow 2CO$	Decomposition $CaCO_3$, Fe_2O_3	Ergun's equation	$H_2O(l) \Rightarrow H_2O(g)$, $H_2+1/2O_2 \Rightarrow H_2O$	Not considered	Obtaining a high-quality agglomerate with a min. return rate due to the genetic optimization method with a min. amount of hydrocarbon
[15]	Development of a wet iron ore agglomeration simulator	2-D	Solid, gaseous,	Unknown	$C+O_2 \rightarrow CO_2$	Decomposition $CaCO_3$	Ergun's equation	Unknown	Not considered	A model for analyzing, optimizing, and

										controlling the process. The model predicts the temperature of the agglomerate and gas, the sintering point.
[10]	3D model for modeling processes in the agglomerate	3-D	Solid, gaseous,	Convection, Thermal conductivity, radiation	$C+O_2 \rightarrow CO_2$ $C + 1/2O_2 \rightarrow CO$ $C+CO_2 \rightarrow 2CO$ $C+H_2O \rightarrow CO+H_2$	Decomposition $CaCO_3$ Fe_2O_3	Modified Ergun equation	CO_2 (g)+ H_2 (g)$\rightarrow CO$(g)+ H_2O(g) H_2O(l) $\leftrightarrow$ H_2O(g)	Consideration of volume fraction, particle diameter and size factor	Demonstration of the 3D behavior of the agglomeration front and the internal temperature distribution
[1]	Development of a model of the agglomeration process using the effects of humidity, condensation and evaporation	1-D	Solid, gaseous,	Convection	Burning of hydrocarbon	Not considered	Unknown	Balance equations for changes in moisture, evaporation, and condensation	Constant	The model predicts the temperature values in the agglomerate
[11]	Predicting agglomerate quality, inchding chemical characteristics and physical strength, performance, and fuel consumption	1-D	Solid, gaseous,	Convection	$(1+\varphi)C + \left(1+\frac{\varphi}{2}\right)O_2 \rightarrow \varphi CO + CO_2$	Decomposition $CaCO_3$ $MgCO_3$	Ergun's equation	Evaporation and condensation	Not considered	Model parameter identification by optimization using temperature measurements and a self-organizing Kohonen map
[17]	Improving the efficiency of the agglomeration process by optimizing the permeability configuration	2-D	Solid, gaseous,	Convection	$C+O_2 \rightarrow CO_2$	Decomposition $CaCO_3$, the sulfation equation	Brinkman equation, where the permeability and Forsheimer coefficients are expressed through the Ergun equation	H_2O(l) $\leftrightarrow$ H_2O(g)	Developed on the basis of measured values of air velocity in the charge and depends on the vertical and horizontal permeability bars	1 and 2-layer horizontal and vertical slats and their influence on the temperature in the agglomerate, the coke residue and the moisture content are considered
[12]	Determining the effect of the growth of granules on the duration of agglomeration and the yield of finished products	2-D	Solid, gaseous,	Convection, Thermal conductivity, radiation	$(1+\varphi)C + \left(1+\frac{\varphi}{2}\right)O_2 \rightarrow \varphi CO + CO_2$ $CO+1/2O_2 \rightarrow CO_2$	Decomposition $CaCO_3$ Fe_2O_3 oxidation Fe_3O_4	The Navier – Stokes equation, where the pressure drop is described by Darcy's law and obeys the Ergun equation in a porous medium	Patinson's model for predicting evaporation CO_2 (g)+ H_2 (g)$\rightarrow CO$(g)+ H_2O(g)	Empirical Castro Equation	Increased sinter yield and reduced thickness of the molten zone by increasing the size of iron ore, which shortens sintering time and increases productivity

Based on the analysis of modern studies of the agglomeration process (Table 1.1), the following conclusions can be drawn:

- most of the reviewed works are devoted to the agglomeration of iron ores, as the most common process, and therefore there is a gap in the study of phosphorite ores. The difference between the sintering process of iron and phosphorite ores lies in the chemical transformations that take place on the sinter machine, as well as operational variables - sintering time, temperature and discharge in vacuum chambers, cake permeability and many other parameters

- the research results are verified with laboratory experiments obtained in the "test pot", the material in which goes through the same stages as the material on the sintering belt. Therefore, the results do not take into account the influence of natural external factors encountered directly in the real process, which makes the results obtained with a laboratory setup ideal. This leads to the need for additional verification of the obtained mathematical models at the plant;

- most of the models do not take into account the effect of porosity change during sintering, which is an important characteristic of the process that affects the rate of gas movement in the charge;

- chemical reactions occurring during the process have a major effect on the temperature of the charge.

Therefore, in order to create an adequate model, it is necessary to carry out a complete analysis of the charge: the melting and solidification temperature, the properties of the components, such as density, heat capacity, viscosity, and others, to create a mathematical model for changing the sinter porosity and to verify data on real objects.

Works on the classical modeling of an object are devoted to the use of equations of temperature change in the solid, gaseous phases and to the heat transfer between them. In this case, the initial charge is a porous material, which implies the possibility of using a heat transfer model in a porous medium. This will allow taking into account both the heat change in solid and gaseous medium, and the changing model of the material porosity.

2 SYNTHESIS OF THE MATHEMATICAL MODEL OF THE AGLOMERATION PROCESS OF PHOSPHORITE ORE

2.1 Object of modeling

The object of modeling is a pallet on which the initial material - charge is supplied. A step signal (step time = 2 min) is used to simulate the gas supply to the pallet under the hearth (average time of the pallet under the hearth). These assumptions are taken on the basis of [2] depending on the speed of the sintering belt. Sinter machine length is 78 m, average speed 3.6 m/min, charge layer height 260 mm.

As can be seen from the literature review, for the agglomeration process modeling, namely, temperature changes during sintering, there are used the physical sintering laws of heat transfer between solid and gaseous medium. It is known that the charge as a result of the sinter roasting process turns into an sinter, which is a lumped material and, in fact, is a porous material.

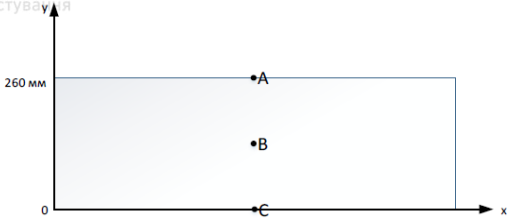

Fig. 2.1. Object of modeling

A porous material is a solid body containing free space in its volume in the form of cavities, channels or pores. The pore sizes, as a rule, are much smaller than the geometric dimensions of the solid body itself.

The initial charge can also be considered as a porous material, since the granules of the charge have a size $(3\text{-}10)\cdot10^{-3}$ m, and the distance between the granules is $(0\text{-}3)\cdot10^{-3}$ m. Therefore, to simulate the temperature change in vacuum chambers in the process of agglomeration, in this work, there is considered a model of heat transfer in a porous material, at which the temperatures of gas and solid material are considered the same. This will reduce the dimension

of the final mathematical model, and speed up the process of modeling and calculation. To determine the correctness of the created model, there will also be created a classical model of heat transfer between the solid and gaseous phases of the sintering process. The simulation results will be presented at points A, B and C (Figure 2.1).

2.2 Schematic representation of the model

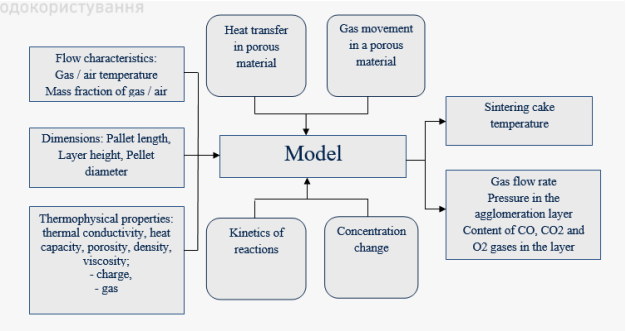

Fig. 2.1. Schematic representation of the model

2.3 Calculation of the temperature change during sintering

Heat transfer in porous material

Heat transfer through a porous medium is usually considered as combined heat fluxes [3], such as heat conduction along its solid matrix, heat radiation through internal pores, and thermal convection or thermal conduction through gases filling the pores. Regarding the last one, there is an inevitable choice between convective and conductive heat flow in pores filled with gas, convective heat transfer is suppressed in pores less than about 10 mm in size. Porous materials have applications across a wide range of engineering and scientific disciplines. The porous material is essentially a two-phase structure - a solid phase and a gaseous (liquid) phase [4]. The initial phosphorite charge, as well as the final sinter, is a porous material in which the solid and gaseous phases are considered. In this case, the temperatures of the solid and gaseous phases in the porous material are equal to $T_s = T_f = T$ and are determined by the following formula

$$\theta\rho_s c_{\rho.s} + (1-\theta)\rho Cp\frac{\partial T}{\partial t} \rho C_s u\nabla T + \nabla(-(\theta k_s + (1-\theta)k\nabla T) = Q, \quad (2.1)$$

where $k[W/(\text{m}\cdot k)]$ - thermal conductivity (gas),

ρ[кг/м^3] – density (gas),

C_p[Дж/(кг·K)] - heat capacity at constant pressure (gas),

γ - specific heat ratio (gas),

θ=(1- porosity) - volume fraction (solid),

$k_s[W/(\text{m}\cdot K)]$ - thermal conductivity (porous matrix),

ρ_s[кг/м^3] - density (porous matrix),

C_{ps} [Дж/(кг·К)] – specific heat (porous matrix) (formula 2.16),

$Q[W/m^3]$ - heat source from chemical reactions (formula 2.13) and heat source supplied from outside,

u - gas velocity in a porous medium (formula 2.7).

Calculation of heat transfer between solid and gaseous media

Heat transfer is the process of transferring heat from one point to another due to a difference in temperature. Heat transfer combines 3 main processes - thermal conductivity (conduction), convection and radiation.

When considering the process of heat transfer occurring during sintering of a charge, there is often considered a model in which two media are considered: solid (charge) and gaseous (agglomerated gases) and heat transfer between them [5].

The solid phase temperature is determined by the following formula

$$\rho_g C_{pg} \frac{\partial T_g}{\partial t} + \rho_g C_{pg} u \nabla T_g - \nabla k_g \nabla T_g = Q + Q_{sg}, \qquad (2.2)$$

where index g indicates the properties of the gaseous phase, Q_{sg} - heat transfer between solid and gaseous phases (formula 2.5). The boundary conditions of all walls correspond to the temperature T_g.

The temperature of the solid component is calculated by the formula

$$\rho_g C_{pg} \frac{\partial T_s}{\partial t} + \rho_s C_{ps} u \nabla T_s - \nabla k_s \nabla T_s = Q + Q_{sg} \qquad (2.3)$$

where index s indicates the properties of the solid phase, Qgs - heat transfer between gaseous and solid phases.

In this case, the temperature in the vacuum chamber is the temperature of the exhaust gases.

Heat transfer between phases according to [21] is calculated by the formula

$$Q_{g \to s} = (T_g - T_s) \frac{\alpha \cdot 6(1-\varepsilon)}{d}$$
$$\alpha = \frac{kg}{d}\left(2 + 0.6\sqrt{\mathrm{Re}}\sqrt[3]{\mathrm{Pr}}\right) \qquad (2.4)$$

where ε - material porosity,

Re - Reynolds number,

Pr - Prandtl number.

Due to the fact that the fraction of the solid phase is not equal to the gaseous one, we introduce this relation into formula (2.4)

$$Q_{gs} = \frac{Q_{g\to s}}{\theta};\;\; Q_{sg} = \frac{Q_{g\to s}}{1-u}. \qquad (2.5)$$

The Prandtl number is determined by the formula [22]

$$Pr = \frac{MC_p}{k}$$

where M - dynamic viscosity of the gaseous phase.

2.4 Determination of the gas movement velocity in a porous medium

Modeling the movement of a gas flow for the sintering process of phosphorite ores has the greatest influence on the speed, temperature of the sintering process and its quality.

One of the new directions for describing the movement of a gas flow during agglomeration is the use of the Ergun equation as part of other equations. The Brinkman equation appeared as a combination of Darcy's law and the Navier-Stokes equation, and describes the slow

flow movement in a porous medium and fast flow in channels. Flow in a saturated porous medium can be modeled using Darcy's law or Darcy-Brinkman model depending on the specific pore size. They allow to find the same variables as the Navier-Stokes equations, but they include terms that take into account the porosity of the medium through which the fluid flows [6]. Then the equations of movement in a porous material can be determined by the Brinkman equation

$$c\frac{\partial u}{\partial t} = \nabla\left[-pI + \text{м}\frac{1}{\in_p}(\nabla u + (\nabla u)^T\right] - \left(\text{м}\,k^{-1} + \text{в}_f|u| + \frac{c\nabla u}{\in_p^2}\right)u \quad (2.6)$$

where k[м^2] - permeability (porous matrix), T[C] - charge temperature (formula 2.1), then, taking into account the Ergun equation, layer porosity, surface roughness and, possibly, the presence of walls [7]

$$k = \left[\frac{150 mu(1-e)^2}{d^2 e^3}\right]^{-1} \cdot \frac{1}{f_p f_{pbase}}, \quad (2.7)$$

$$b_f = \frac{1{,}75 cu^2(1-e)}{de^3} \cdot \frac{1}{f_p f_{pbase}}, \quad (2.8)$$

where f_p - porosity change factor during sintering shrinkage, f_{pbase} - the global calibration constant in the Ergun equation = 3.5.

2.5 Determination of heat resulting from combustion of coke

The agglomeration process is accompanied by the release of heat due to the combustion of coke. In this case, during the combustion of coke, only part of the coke is oxidized to carbon dioxide, the other part is oxidized to carbon monoxide. The high temperature in the layer leads to the fact that most of the monoxide is oxidized to carbon dioxide [8]. When burning coke, the following chemical reactions are usually considered

$$\begin{aligned} &C + O_2 = CO_2, \\ &C + 0{,}5\,O_2 = CO, \\ &0{,}5\,C + 0{,}5\,CO_2 = CO, \\ &C + H_2O = CO + H_2. \end{aligned} \quad (2.9)$$

The kinetics of reactions according to [44] depends on the concentration of carbon monoxide, oxygen and water in gas.

$$R_j = k^f \prod c_i^j, \quad (2.10)$$

where k^f - reaction rate constant determined by the Arrhenius equation

$$k^f = A^f \exp\left(\frac{-E^f}{R_g T}\right), \quad (2.11)$$

where A^f - frequency coefficient, $E^f[j/mol]$ - activation energy, R_g - universal gas constant. The coefficients are determined according to [7].

Then the heat released by the reaction is determined by the formula

$$Q_j = -R_j H_j, \quad (2.12)$$

where H_j - enthalpy.

2.6 Change in concentration due to combustion reaction

The change in gas concentration in equation (2.12, 2.13) is determined

$$c_i = \frac{\rho\omega_i}{M_i}, \tag{2.13}$$

where ω_i - mass fraction of gas i

$$\varepsilon\rho\frac{\partial\omega_i}{\partial t} + \nabla j_i + \rho(u\cdot\nabla)\omega_i = R_i, \tag{2.14}$$

where j_i - variable containing the diffusion model of the process, R_i - reaction rate (formula 2.13).

2.7 Determination of thermo physical properties of the charge

The thermo physical properties (TPP) of ore materials require numerous experiments, since the samples differ in the multicomponent mineral and chemical composition and, at the same time, individual components undergo chemical changes at elevated temperatures. The composition of the initial charge includes carbonate phosphorites (P_2O_5 content = 18-25%) and coke. Data on heat capacity, thermal conductivity, density can be determined from various reference books [9-12]. Then the thermophysical properties of the charge (thermal conductivity k_s, heat capacity $c_{p.s}$, density ρ_s) can be determined as follows [13]

$$k_s = \sum\omega_{s.i}k_{s.i};\quad c_{\rho.s} = \sum\omega_{s.i}c_{\rho.s.i};\quad \rho_s = \sum\omega_{s.i}\rho_{s.i}, \tag{2.15}$$

where $\omega_{s.i}$ - mass fraction of charge component

The thermal conductivity of individual components in the structure of phosphorites was obtained from experimental data for a wide range of mineralogical composition of phosphorites by the method of nonlinear least squares.

2.8 Agglomeration process modeling

The possibility of using the physical law of heat transfer of a porous material for the agglomeration process is tested through standard models of heat transfer in the gaseous and solid phases, presented in many works on the study of the agglomeration process.

First of all, the form of the temperature curves at the points of the charge A, B and C (Figure 2.1) and the velocity of the gaseous phase inside the sinter is determined. Since the main parameter characterizing sintering is temperature, it is necessary to calculate the temperature for models of heat transfer between solid and gaseous media, and heat transfer in porous material at points A, B and C (Figure 2.3 - Figure 2.5). The gas velocity inside the agglomeration cake at point B is shown on Figure 2.6.

Since the temperature during the agglomeration process moves from top to bottom due to the vacuum chambers located under the sintering belt, the main parameter responsible for layer sintering is the temperature in the vacuum chamber (point C). Therefore, it is advisable to calculate the root-mean-square error between 2 models at point C

$$RMCE = \sqrt{\frac{\sum_{t=0}^{n}\left(T_g^t - T^t\right)^2}{n}} = 3{,}85C$$

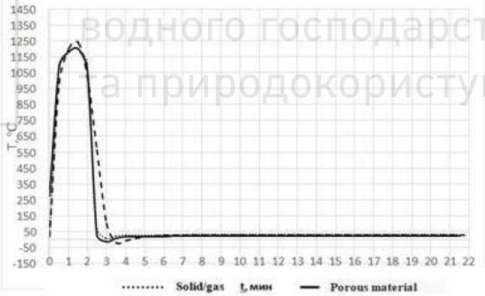

Fig. 2.3. Temperature at point A

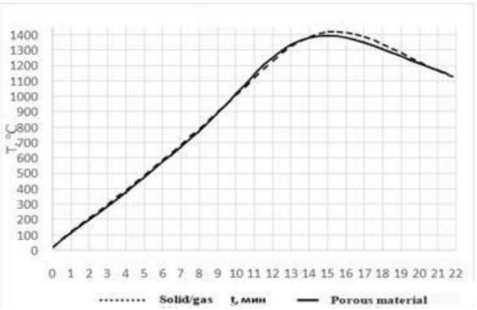

Fig. 2.4. Temperature at point B

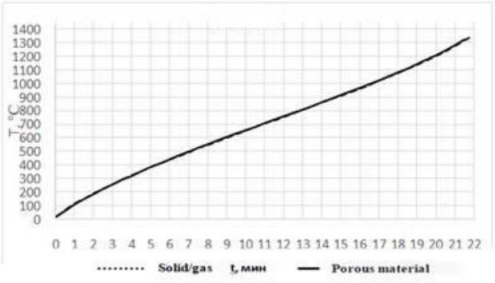

Fig. 2.5. Temperature at point C

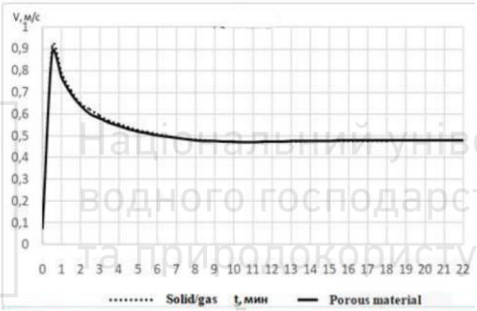

Fig. 2.6. Velocity of the gas phase at point B

As can be seen from the graphs (Fig. 2.3-Fig. 2.6), the use of the physical laws of heat transfer in a porous material for agglomeration process modeling practically does not differ from heat transfer modeling between solid and gaseous media. The root-mean-square error at a temperature of 1350 °C is less than 4 ℃ with the same initial parameters of the charge. Also, the use of a heat transfer model in porous materials makes it possible to reduce the dimension of the system of partial differential equations, which leads to a lighter model and to a reduction in modeling resources, both for setting up the model, connections with other physical processes, and resources for computing (solving) the model.

3 THE CURRENT STATE OF SYNTHESIS METHODS OF CONTROL SYSTEMS OF THE SINTERING POINT DURING SINTER ROASTING

3.1 Predictive models of the sintering point of the charge

One of the key indicators of the sintering quality is the sintering point, which indicates the end of the agglomeration process, and is the point with the highest temperature. Often the sintering point is determined by the operator and based on this prediction, the need to change the output process variables is determined. With the rapid development of prediction methods, there have appeared a huge number of systems that allow prediction the sintering point based on historical data and data from the current process, as a result of which the productivity of the process increases and the quality of the finished product improves.

The problem of predicting and controlling the sintering point has been studied in many works using various algorithms, such as neural networks, genetic algorithms and fuzzy control. Due to the development and widespread use of neural networks, a large number of works, related to prediction, use this method in various areas of research. In the problem of controlling the sintering point of the agglomeration process, *neural networks* have been assigned a huge layer of work. So, for example, in [14], the parameter introduced by the authors - the mathematical bend point of the temperature curve of sinter gases measured in the middle of the sintering belt - is fed at different times to the input of a multilayer neural network, the output of which predicts the sintering point values 5 steps ahead. The predicted error of this model was 0.15, when training the network on a sample of 600 data groups. The neural network is also used in [15], where the values of the sintering belt speed and the position of the sintering point at the previous time instants are fed to its input. The network, together with the training algorithm, is used to update the parameters of the sintering point model, thus forming the neural network identifier used in the adaptive pole (position) finding method. In [16], for intelligent control of the agglomeration process of iron ores, there are fed up data on the current position of the sintering point, the temperature in the middle and the end of the process and the sintering belt speed to the neural network input, the

result is the sintering point prediction. Fuzzy neural networks are also used to predict the sintering point in [17], where the temperatures in the vacuum chambers are selected as input variables and the sintering point as the model output. The neural networks used by the authors in [18] for the synthesis of the model of the sintering point of iron ores are trained on a set of 10,000 data. The dataset includes process parameters (sintering belt speed, ignition temperature, layer height, layer permeability, return, fuel and moisture) and ratio parameters (return, fuel and moisture, limestone, ore, etc.). The prediction result and real values of the sintering point are then fed to a multilinear regression model in order to compensate the neural network error. In this case, the maximum prediction error was 1.3 m. A neural network trained using fuzzy sets is presented in [19] for predicting the sintering point. The input of the neural network is a sample of 80 values of the temperature under the sintering belt, the speed of the sintering belt and the parameter associated with it. The first layer of the network represents inputs, the second layer is responsible for linguistic meaning and is used to calculate the membership function of each component, each node of the third layer represents fuzzy rules, the last layer is the output of the network.

Some works use 2 predictive models of the sintering point: temporal and technological. So, in order to predict the permeability of lead-zinc ores in [20], 6 previous permeability values are fed to the input of a temporary neural network, and for a technological neural network, the input is the fire temperature, humidity, sulfur, lead, silicon dioxide, and speed. In [21], the grey model GM (1,1) of the sintering point of lead-zinc ores is used as a time sequence, and the parameters of the charge permeability and pallet speed are fed to the input of the technological neural network. In [22], to predict the sintering point of iron ores, they also use the integration of the gray model and neural networks. The result of the gray model calculation (gas temperature in the vacuum chambers) is one of the inputs of the backpropagation neural network, along with the sinter machine speed and the sintering belt position at the sintering point at the current time. Authors of works with two predictive models use a fuzzy expert controller that maintains the desired position of the sintering point within the specified boundaries.

In [23], there are presented an optimization model of coke efficiency and a fuzzy controller of the sintering point. The main idea is to improve coke efficiency using an intelligent integrated sintering point control strategy. The sintering belt speed resulting from the optimization model and the output of the fuzzy sintering point controller is integrated using the fuzzy satisfaction method that calculates the final sintering belt speed. The sintering point prediction model developed in [24] also uses 2 models. The temperatures in the vacuum chambers are fed to the sintering point model (first model) to predict the sintering point position. The predictive sintering point temperature model (second model) uses the sintering point temperatures obtained in the previous steps. The results of both models - the position and temperature of the sintering point - together with the sintering belt speed are used as input variables to a robust fuzzy controller, which is based on an improved model of the Takagi-Sugeno linear parameter variation.

In addition to the standard neural network training algorithms, genetic algorithms are used to optimize the value of the neural network weights. Thus, in [25], an adaptive genetic algorithm was used for the control system of the sintering point during the sintering of iron ores, where the input layer of the neural network is the parameters of the initial material, density, sintering belt speed and ignition temperature, and the output layer is responsible for the temperature and pressure of agglomeration gases and gases in a vacuum chamber. The genetic neural network was used for the system for predicting the sintering point of iron ores and in [26], where 707 groups of data obtained as a result of *clustering* and classification of temperature and pressure vectors from 18 vacuum chambers, were fed into the input. The entire system of adaptive structural clustering used methods of spatial clustering of the initial data, a self-organizing neural network map for extracting data relevance properties and a Kohonen map for training the LVQ network.

The idea of clustering was also used in [27] to synthesize a model for predicting the sintering point of iron ores. The K-means clustering module, at the input of which the model of the permeability of the cold charge, the values of the ignition temperature and the coke residue is fed to, is used to form clusters.

The predictive model in this work *does not use neural network algorithms*, and the resulting clusters are fed to the input of the dynamic temperature and vacuum model. The dynamic model is created using a new genetic programming algorithm. An algorithm based on genetic algorithms for optimizing the prediction model of the final sintering based on the support vector machine is presented in [28].

Models that do not use neural networks to predict the sintering point are based *on equations for the temperature or sintering time change*. For example, in [29], the predicted value of the sintering time is determined by the least squares method based on historical data and, depending on the signal of the event model, which determines the time until the end of the pallet movement, the sintering belt velosity is controlled. The event-driven control model over the sintering point of iron ores is presented as a linear, time-constant discrete model in the state space, using the idea of breaking the continuous model into discrete events. The authors of [30] use a curve fitting method and present the result as a cubic curve and a 5 degree curve near the sintering point position. In [31], there is used a parabolic model of the change in the temperature of the sintering point control, compiled from the measured values in three vacuum chambers. It is used to determine the volume of sinter gases and to correct the main signal - the volume of sinter gases, calculated from the volume of oxygen, moisture, and data on the composition of the charge. In [32], there is considered a two-level hierarchical control system for the sintering point and the vertical sintering rate of the agglomeration process of iron ores. The model of the sintering point proposed by the authors is a piecewise-quadratic dependence of the temperature on the position on the sintering belt, which is used when the process is unstable. With a stable sintering process, the vertical sintering rate is calculated using historical data on sintering belt speed and charge height. In [33], the sintering point was approximated using a quadratic function of the output gas temperature. At the same time, a dynamic model of the state space is created to obtain the temperature of the output gases, which uses 6 input variables: the thickness of the charge layer, the speed of the pallets, the pressure in the vacuum chambers and the temperatures of the output gases in the three previous vacuum chambers. A grid

search algorithm optimizes variables within specified limits using a scoring function that provides more accurate temperature prediction results.

The neural network is also not used in [34], where the position control of the sintering point of iron ores is divided into 2 parts: a closed identification model and a generalized predictive control model. In the first part, on the basis of an autoregressive exogenous model, to the input of which the values of the sintering belt speed, amount of moisture, the charge height, volume of air and vacuum are supplied, the position of the sintering point is calculated. Here is used the method of a closed identification system, which serves to dynamically determination of the model parameters. In the second part, based on the transfer function obtained from the identification model, the sintering point is predicted to control the sintering belt speed. In [35], the degree of influence of 4 parameters on the sintering point - pressure in vacuum chambers, air volume, sintering belt speed and ignition temperature - is determined using the optimization algorithm of a swarm of particles.

Naturally, the current position of the sintering point depends on its previous values. This idea was used in the study [36] and analyzed the trends of the time series for the sintering point, which made it possible to use the global and local variables of the trend function. These variables were used as input to the fuzzy controller created on the basis of the operator's knowledge. The output of the controller is the speed of the sintering belt to maintain the sintering point in the required position. The position of the sintering point was also predicted using the “particle swarm” optimization algorithm [37], where the value of 4 influencing parameters: vacuum, incoming air flow, sinter machine speed and ignition temperature were determined using the algorithm.

Based on the literature review, the following conclusions can be drawn:

- in order to predict the sintering point, there are used data on (1) vertical sintering rate, determined by the volume of sinter gases, discharge, properties of the initial material, permeability, charge height, etc.; on (2) temperature in vacuum chambers or sinter gases; on (3) the speed of the sintering belt; on (4) the previous values of the sintering points;

- in order to create predictive models, a large volume of the initial sample is used to obtain accurate models;

- the sintering point is controlled by changing the speed of the sintering belt.

4 MATHEMATICAL MODEL FOR PREDICTING SINTERING POINT

4.1 Main parameters of the predictive model of the sintering point

The amount of return during sintering reaches 40-50%, since the process is controlled only at the end of the sinter machine by the operator's decision, based on a visual assessment of the sinter cut. The return rate needs to be reduced by predicting and controlling the sintering point based on real-time data. The agglomeration process includes many parameters that influence the sintering point. In the work, data measured in real time were used as the main parameters for creating predictive models - the temperature in the vacuum chambers and the gas velocity, determined through the measured value of the pressure (discharge) in the vacuum chambers.

The main predictive variable is the temperature at the bottom of the sintering belt (temperature in the vacuum chambers). Temperature curves (Figure 2.5) represent data samples taken at different times in different initial conditions: different composition of the charge, amount of coke, pressure, but at a constant speed, so they are displayed on the graph only until the desired temperature is reached to determine the actual duration of the process. Additionally, the value of the pressure drop Δp is measured (the difference between the pressure in the upper and lower parts of the charge) and according to the Ergun equation (2.6) the gas velocity u (Figure 2.7) in the upper part of the charge is calculated. The porosity value is calculated according to the method proposed in [38].

4.2 Grey systems for sintering point prediction

The creation of a data collection system with its storage, analysis and constant retraining requires huge time and financial resources. Also, collecting the initial sample, training and creating an effective system requires constant interruption of the production process, which affects its efficiency. In the process under consideration, there

is no full-fledged data collection system, therefore, in order to obtain data, additional measurement systems were used that were not included in the main control circuit. In such conditions, it becomes necessary to use models that require a small amount of the initial sample for training and creating a predictive model. Grey systems theory satisfies these requirements [39].

The grey model of a type GM (1,1) is the most widely used model in the literature and is referred to the first order grey model with one variable. The model is a temporal predictive model with time-varying coefficients. In other words, the model is updated when new data becomes available to the predictive model. Grey GM (1,1) model can only be used with non-negative original samples.

In order to create a grey model GM (1,1) based on the original sample (4.4) and 1-AGO sample (4.5), the generated mean sequence has the following form [40]

$$Z^{(1)} = \left\{Z^{(1)}(1), Z^{(1)}(2), ..., Z^{(1)}(r)\right\}, \quad (4.1)$$

where $Z^{(1)}(k)$ - mean value of adjacent data

$$Z^{(1)}(k) = 0{,}5X^{(1)}(k) - 0{,}5X^{(1)}(k-1).$$

The sequence of calculating the least squares of the grey differential equation GM (1,1) is determined as follows

$$X^{(0)}(k) + aZ^{(1)}(k) = b$$

Then, the whitening equation has the form

$$\frac{dX^{(1)}(t)}{dt} + aX^{(1)}(t) = b, \quad (4.2)$$

where $[a,b]^{\mathrm{T}}$ - a sequence of parameters which can be found as follows

$$[a,b]^T = (B^T B)^{-1} B^T Y, \quad (4.3)$$

$$Y = [X^{(0)}(2), X^{(0)}(3), ..., X^{(0)}(r)]^T$$

$$B = \begin{bmatrix} -Z^{(1)}(2) & 1 \\ -Z^{(1)}(3) & 1 \\ -Z^{(1)}(r) & 1 \end{bmatrix}.$$

The solution of equation (4.8) $X^{(1)}(t)$ at the moment of time k

$$X_p^{(1)}(k+1) = \left[X^{(0)}(1) - \frac{b}{a}\right]e^{-ak} + \frac{b}{a}.$$

To obtain predicted values at the time (k+1), there is used IAGO

$$X_p^{(0)}(k+1) = \left[X^{(0)}(1) - \frac{b}{a}\right]e^{-ak} + \frac{b}{a}(1-e^{a}).$$

Most of the systems are generalized energy systems. They will follow a grey exponential law if they are not violated by any other factors, and then they can be accurately predicted by GM's grey predictive model (1, 1). Actual systems will be more or less influenced by other factors and will never fully follow the grey exponential law, so it is important to consider grey system models that take other influencing factors into account.

The influence of several factors on the predicted value for grey models can only be considered on the basis of modifications of the GM (1,n) model, which is clearly demonstrated in [41]. The continuous integral grey convolution model GMC (1,n) [42] is one of the main models with (n-1) influencing factors. Based on this model, other continuous linear gray models with (n-1) influencers have been developed. For example, the interval model with the convolution integral IGDMC (1,n) [43] is designed to predict the interval in which the variable is located. The FGMC (1,n) model [44] was developed on the basis of the idea of independence of the prediction from the first pair of initial data in the sample. The deterministic grey model with convolution integral DGDMC (1,n) [45] differs from GMC (1,n) in the estimate of the first derivative and parameters: the first derivative is estimated numerically by the cubic spline curve and model parameters, in accordance with the deterministic convergence scheme. The error in the strength prediction considered by Thien is 0.54% for FGMC (1,n), 1.25% for GMC (1,n), 1.85% for DGDMC (1,n) and 2.4% for IGDMC (1,n). Later in [46], there was shown an optimized model GDMC (1,n) - OGDMC (1,n), in which the value of the grey derivative $dX_1^{(1)}(t)\ \ (t)/dt$ is not determined by the weighted average value $X_1^{(1)}(t)\ \ X^{(1)}(t)$ и $dX_1^{(1)}(1)dX\ dX_1^{(1)}(t-1)$, but through the weight coefficient ρ_i determined using the particle swarm algorithm [47]

$$c_i X_i^{(1)}(t) - (1-c_i)X_i^{(1)}(t) \qquad (4.4)$$

Here, the value of the root-mean-square error as a percentage to the a prior sampling period (RMSPEPR) in OGDMC (1,*n*) decreased 3.8 times - from 7.07% to 1.86%. in order to select the most accurate model for predicting the sintering point in a vacuum chamber, we will conduct experiments using the FGMC (1,*n*), GMC (1,*n*) and GDMC (1,*n*) models, which have the lowest prediction error.

4.2.1 Continuous integral gray convolution model GMC (1,2)

The gas velocity calculated from the known pressure Δp measured in real time was chosen as the influencing factor. The continuous integral gray model GMC (1,2) with one influencing factor is a linear differential model

$$\frac{dY^{(1)}(t)}{dt} + b_1 Y^{(1)}(t) = b_2 X^{(1)}(t) + u \qquad (4.5)$$

where $Y^{(1)}(t)$ and $X^{(1)}(t)$ represent 1-AGO data

The gray derivative for the AGO data of the first order in (4.12) is traditionally represented as

$$Y^{(1)}(t) = \sum_{l=1}^{t} Y^{(0)}(l), X^{(1)}(t) = \sum_{l=1}^{t} X^{(0)}(l). \qquad (4.6)$$

The gray derivative for the AGO data of the first order in (4.12) is traditionally represented as:

$$\frac{dY^{(1)}(t)}{dt} = \lim_{\Delta t \to \infty} \frac{Y^{(1)}(t+\Delta t) - Y^{(1)}(t)}{\Delta t} = Y^{(1)}(t+\Delta t) - Y^{(1)}(t), \qquad (4.7)$$

with $\Delta t \to 1$.

The parameters (4.12) are determined using the least squares method (4.9)

$$\left[b_1, b_2, u\right]^T = (B^T B)^{-1} B^T Y_R, \qquad (4.8)$$

where *t* varies from 1 to *r*, representing the volume of the initial sample to build the model in (4.12),

$$B = \begin{bmatrix} -0{,}5(Y^{(1)}(1) + Y^{(1)}(2)) & -0{,}5(X^{(1)}(1) + X^{(1)}(2)) & 1 \\ -0{,}5(Y^{(1)}(2) + Y^{(1)}(3)) & -0{,}5(X^{(1)}(2) + Y^{(1)}(3)) & 1 \\ -0{,}5(Y^{(1)}(r-\dot{1}) + Y^{(1)}(r)) & -0{,}5(X^{(1)}(r-\dot{1}) + X^{(1)}(r)) & \dot{1} \end{bmatrix} \qquad (4.9)$$

$$Y_R = \left[Y^{(1)}(2), Y^{(1)}(3), \ldots, Y^{(1)}(r)\right]. \qquad (4.10)$$

The forecast of the agglomerate temperature $\hat{0}$ is determined by the following equation

$$\hat{Y}^{(0)}(t) = \hat{Y}^{(1)}(t) - \hat{Y}^{(1)}(t-1). \quad (4.11)$$

$$\hat{Y}^{(1)}(t) = \hat{Y}^{(0)}(1)e^{-b_1(t-1)} + \tfrac{1}{2}e^{-b_1(t-1)} \times (b_2 X^{(1)}(t) + u) + \tfrac{1}{2}b_2 X^{(1)}(t) + u) + \textstyle\sum_{i=2}^{t-1} e^{-b_1(t-i)} \times (b_2 X^{(1)}(i) + u). \quad (4.12)$$

4.2.2 Continuous integral gray convolution model of the first pair of FGMC data(1,*n*)

The differential equation of the gray prediction model FGMC (1,*n*), presented in [44], is the same as for GMC(1,*n*), but is modeled by data that includes information from the first pair of source data.

The parameters (4.12) are determined by the least squares method (4.15), where

$$B = \begin{bmatrix} -0{,}5(Y^{(1)}(1) + Y^{(1)}(2)) & -0{,}5(X^{(1)}(1) + X^{(1)}(2)) & 1 \\ -0{,}5(Y^{(1)}(2) + Y^{(1)}(3)) & -0{,}5(X^{(1)}(2) + Y^{(1)}(3)) & 1 \\ -0{,}5(Y^{(1)}(r-\dot{1}) + Y^{(1)}(r)) & -0{,}5(X^{(1)}(r-\dot{1}) + X^{(1)}(r)) & \dot{1} \end{bmatrix} \quad (4.13)$$

$$Y_R = [Y^{(1)}(1), Y^{(1)}(2), \ldots, Y^{(1)}(r)]. \quad (4.14)$$

The forecast of the agglomerate temperature is determined according to the following equation

$$\hat{Y}^{(0)}(t) = Y^{(0)}(0)e^{-b_1 t} + u(t-1)\textstyle\sum_{i=1}^{t}\frac{1}{2} e^{-b_1(t-i+0{,}5)}\left(b_2(X^{(1)}(i) - X^{(1)}(i-1)\right). \quad (4.15)$$

Optimal continuous dynamic integral gray convolution model OGDMC (1,*n*)

Differential equation of the gray dynamic model with the convolution integral.

$$\frac{dY^{(1)}(t)}{dt} + b_1 Y^{(1)}(t) = b_2 + \textstyle\sum_{i=2}^{n}\left(b_{2i-1}\frac{dX^{(1)}(t)}{dt} + b_{2i}X^{(1)}(t)\right) \quad (4.16)$$

The parameters (4.23) for the continuous dynamic integral model are determined using the least squares method (4.14), the YR vector is calculated by (4.21) and

$$B = \begin{bmatrix} -0{,}5(Y^{(1)}(1) + (Y^{(1)}(2) & 1 & X^{(0)}(1) & -0{,}5(X^{(1)}(1) + (X^{(1)}(2) & 1 \\ -0{,}5(Y^{(1)}(2) + (Y^{(1)}(3) & 1 & X^{(0)}(2) & -0{,}5(X^{(1)}(2) + (X^{(1)}(3) & 1 \\ -0{,}5(Y^{(1)}(r-\dot{1}) + (Y^{(1)}(r) & \dot{1} & X^{(\dot{0})}(r) & -0{,}5(X^{(1)}(r-1) + (X^{(1)}(r) & \dot{1} \end{bmatrix} \quad (4.17)$$

To obtain the parameters of the optimal model of the gray value of the derivative dX(1)(t)/dt and dY(1)(t)/dt is not determined by the

weighted average value of X(1)(t) and dX(1)(t-1), Y(1)(t) and dY(1)(t-1), respectively , and using a weighting factor of PI, defined by using the particle swarm optimization algorithm according to equation (4.11).

Forecast of the sinter temperature is defined by (4.18), where

$$\hat{Y}^{(1)}(t) = Y^{(0)}(1)e^{-b_1(t-1)} + u(t-2)\sum_{\tau=2}^{t}\frac{1}{2}e^{-b_1(t-i+0,5+0,5\lambda_1)} \times \left[\frac{1}{2}(f(\tau)-(f(\tau-1))+\frac{1}{2}\lambda_1(f(\tau)-(f(\tau-1))\right]+\frac{1}{2}e^{-b_1(t-i+0,5+0,5\lambda_2)} \times \left[\frac{1}{2}(f(\tau)-(f(\tau-1))+\frac{1}{2}\lambda_1(f(\tau)-(f(\tau-1))\right] \quad (4.18)$$

where $\lambda_1 = -\frac{1}{\sqrt{3}}$, $\lambda_2 = -\frac{1}{\sqrt{3}}$

$$f(t) = b_2 + \sum_{i=2}^{n}(b_{2i-1}X^{(0)}(t) + b_{2i}X^{(1)}(t) \quad (4.19)$$

4.3 Results of predictive models

The root mean square error in percent (RMSPE) of predictive models for 3 samples is presented in Table 4.4, where the initial sample size *r* for building the model includes data from the beginning of the sintering process to 7.5 minutes. (15 values). The results of the predictive models for each sample are shown in Table 4.4.

Table 4.4

RMSPE gray models

№	RMSPE, %		
	GMC(1,n)	FGMC(1,*n*)	GDMC(1,*n*)
1	2.2413	4.1062	2.6575
2	1.6697	3.4544	3.6921
3	1.0952	3.8123	4.1833

The best result of prediction of the sintering point of the charge was obtained as a result of using the GMC (1,*n*) model, the largest error of which is 2.2% versus 4% for other types of models.

Predictive GMC (1,*n*) models for 3 samples are presented in Table 4.5, where the volume of the initial sample for creating the model includes data from the beginning of the sintering process to 7.5 minutes (15 values). The parameters of the grey model, which were found using equation (4.15), differ significantly for each sample. This is due to the fact that each temperature curve was obtained under different initial conditions: the content of coke,

phosphorite ore, the amount of return, moisture and other parameters of the charge, which are not directly accepted for creating a predictive model. Moreover, during production under real conditions, it is impossible to continuously monitor the composition of the charge, which makes it difficult to use a model that takes into account all factors. Therefore, it is necessary to create a predictive model that uses only the parameters measured in real time and dynamically creates a predictive model for a specific batch of sintered ore. The prediction results based on grey systems do not improve the accuracy compared to other models presented in the literature earlier, but it allows to create an adequate predictive model of the sintering point in the absence of a large amount of historical data. An additional advantage of the model is the reduction in the time spent on collecting initial data and training the model.

Table 4.5

Built GMC Models

Samsung	GMC(1,в)	RMSPE,%
1	$\frac{dY^{(1)}t}{dt} - 0{,}0011762481\ Y^{(1)}(t) = = 55.0012859\ ^{(1)}X(t) + 41.90354212$	2,2413
2	$\frac{dY^{(1)}t}{dt} - 0{,}0030327\ Y^{(1)}(t) = = 62.1579506\ X^{(1)}(t) + 41.27688268$	1,697
3	$\frac{dY^{(1)}t}{dt} - 0{,}00575793\ Y^{(1)}(t) = = 47.8204758\ X^{(1)}(t) + 36.486036$	1,0952

4.4 Optimal gray predictive model of the OGMC sintering point(1, *n*)

To improve the accuracy of the predictive model GMC (1,*n*), instead of the weighted average for determining the gray derivative, we introduce the coefficient pϵ [0; 1], then (4.16) takes the following form

$$\begin{bmatrix} -(1-\rho)Y^{(1)}(1)+\rho Y^{(1)}(2) & (1-\rho)X^{(1)}(1)+\rho X^{(1)}(2) & 1 \\ -(1-\rho)Y^{(1)}(2)+\rho Y^{(1)}(3) & (1-\rho)X^{(1)}(2)+\rho X^{(1)}(3) & 1 \\ -(1-\rho)Y^{(1)}(r-1)+\rho Y^{(1)}(r) & (1-\rho)X^{(1)}(r-1)+\rho X^{(1)}(r) & 1 \end{bmatrix} \quad (4.20)$$

The coefficient ρ is determined by the swarm of particles optimization method [62]. In 1995, J. Kennedy and R. Eberhart proposed a method for optimizing continuous nonlinear functions called the particle swarm algorithm [62]. The current state of the particle is characterized by coordinates in the space of solutions (that is, in fact, the solution associated with them), as well as the velocity vector. Both of these parameters are randomly selected during the initialization phase. In addition, each particle stores the coordinates of the best solution found for it, as well as the best solution passed by all particles - this simulates instant information exchange between birds.

At each iteration of the algorithm, the direction and length of the velocity vector of each of the particles change in accordance with the information about the found optima. The particle swarm algorithm is a system of particles that move to optimal solutions, each particle contains the coordinates of the found best solution (*pbest*) and the best solution of all particles in the swarm (*gbest*). The direction and length of the particle velocity vector is determined by the following formula

$$\vartheta_i = \vartheta_i + a_1 rnd()(pbest_i - x_i) + a_2 rnd()(gbest_i - x_i) \quad (4.21)$$

where ϑ_i - particle velocity vector, a_1, a_2 - constant accelerations, a x - particle current position. In this case, the current position of the particle determines the value of the coefficient ρ.

Minimum (4.26) is used as an optimality criterion. The resulting predictive models and *RMSPE* for the period after the training sample are presented in Table 4.6, where it can be seen that the accuracy of the grey model has improved.

In [46], the interpolation coefficients ρ_i are introduced into the values of each of the variables in GDMC (1,n). Application of this algorithm to the GMC (1,n) model will have the following changes in (4.15)

$$\begin{bmatrix} -(1-\rho_1)Y^{(1)}(1)+\rho_1 Y^{(1)}(2) & (1-\rho_2)X^{(1)}(1)+\rho_2 X^{(1)}(2) & 1 \\ -(1-\rho_1)Y^{(1)}(2)+\rho Y_1^{(1)}(3) & (1-\rho_2)X^{(1)}(2)+\rho_2 X^{(1)}(3) & 1 \\ -(1-\rho_1)Y^{(1)}(r-1)+\rho_1 Y^{(1)}(r) & (1-\rho_2)X^{(1)}(r-1)+\rho_2 X^{(1)}(r) & 1 \end{bmatrix} \quad (4.22)$$

The prediction results have changed insignificantly (Table 4.7), but the time to find the optimal values of the ρi coefficients has increased. An increase in (n-1) dependent variables leads to an optimization time that increases exponentially, and makes it difficult to use an algorithm with different coefficients for each variable in real-time control.

Therefore, in order to improve the accuracy of modeling and prediction, there is used the coefficient ρ for the control task. The prediction results for OGMC (1,n) are presented on Figures 4.7-4.9 in comparison with GMC (1,n) and the original sample.

The grey model coefficients (Table 4.7), which were found by (4.15), differ significantly for each sample.

This is due to the fact that each temperature curve was obtained under different initial conditions: the content of coke, phosphorite ore, the rate of return, moisture content and other parameters of the charge, which were not directly taken to create the predictive model.

Moreover, during production under real conditions, it is impossible to continuously monitor the composition of the charge, which makes it difficult to use a model that takes into account all factors.

Therefore, it is necessary to create a predictive model that uses only measured real-time factors and dynamically creates a predictive model for a specific batch of sinter ore.

Table 4.7

Results of the optimal GMC (1,n) model

№	Коэффициенты	GMC(1,n) ρ	RMSPE ρ, %	GMC(1,n) ρ_i	RMSPE ρ_i, %
1	ρ	0.2261	1.2120	0&0.2283	1.2110
	b_1	-0.0005		-0.0005	
	b_2	56.3769		56.3554	
	u	28.3447		28.4573	
2	ρ	0.3669	1.4266	1&0.3683	1.4249
	b_1	0.0003		0.0003	
	b_2	58.9057		58.8892	
	u	30.6943		30.7584	
3	ρ	0.4193	0.9756	1&0.4384	0.9588

b_1	0.0025		0.0023	
b_2	62.1686		61.9513	
u	37.5064		38.5224	

5 STRUCTURE OF THE CONTROL SYSTEM BASED ON PREDICTIVE MODEL

Dynamic creation of a grey model assumes the use of only actual data obtained in real time about the sintering process, while the model does not depend on historical data and allows to predict the value of the charge temperature at the end of the sintering belt. If the predicted

temperature of the charge at the extreme point does not reach the specified value, the agglomeration process must be controlled. Control can be performed by changing the amount of fuel in the initial charge, the speed of the sintering belt and the pressure created in the vacuum chambers. A change in the amount of fuel affects only the part of the charge that has not yet been fed to the sinter, therefore this effect is not taken into account in the work.

The proposed control structure for the sintering point (Figure 5.1) includes:

1 Collecting data on temperature and pressure in vacuum chambers from the beginning of the process to a certain point.

2 Creation of the optimal grey predictive model OGMC (1,n) based on the accumulated data.

3 Prediction of the temperature to the end of the sintering belt.

4 Optimization of the process control parameters (speed and pressure in the vacuum chambers) to achieve the desired temperature at the end of the process.

5 Modification of control parameters for the batch under consideration to obtain good sinter quality and minimum return.

The control structure has the following algorithm: after the charge enters the hearth, the system starts collecting data on temperature, pressure in the vacuum chambers and sintering belt speed. Based on the collected data, there is created an optimal grey predictive model OGMC (1,n), which predicts the temperature value at the end of the sintering belt. If the temperature does not correspond to the sintering

point of the sinter, then the predictive optimization algorithm calculates the required values of the sintering belt speed and pressure in the vacuum chambers. These calculations are fed to the corresponding controllers. After the charge reaches the end of the sintering belt, the cycle is repeated.

The particle swarm method is used [47] as a predictive optimization method. It is implemented as follows:

1 There are generated *m*-particles (m=2) in n-dimensional space. The position and velocity of the particle are represented as $x_i=(x_{i1}; x_{i2};...; x_{in})$ and $\vartheta_i=(\vartheta_{i1}; \vartheta_{i2};...;\_\vartheta_{in})$, where i=1;...;m. The current position of the particle x (4.27) includes two variables: the sample size, from which the duration of the agglomeration process is calculated and the gas velocity.

2 Initial position of the particle *xi* and particle velocity ϑ_i are generated randomly and within specified limits: $t_{min}\leq x_1\leq t_{max}$, $X_{min}\leq x_2\leq X_{max}$, where t - time step, X - discharge in vacuum chambers.

3 According to (4.14) x_2 is substituted into matrix B and according to (4.17) x_1 is substituted as a parameter t.

4 The fitness function (4.26) is calculated for each particle

5 The value of the fitness function of each particle is compared with the best solution of all the particles in the swarm *pbest* to correct the value, if the value is optimal, then it is taken as the best position of the particle, if not, then the transition to the next step occurs.

6 Calculation of the particle velocity and position according to equation (4.27).

7 When the criterion for the end of the algorithm is reached, the result and its fitness function are determined, which correspond to the optimal parameters and RMSPE, otherwise the transition to step 3 occurs.

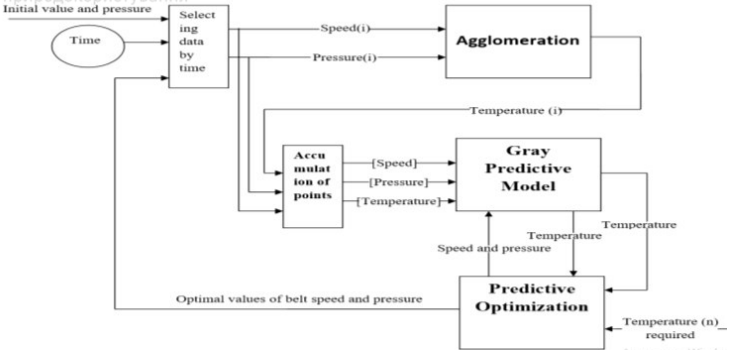

Fig. 5.1. Control system for the point of the cake

Using the obtained value of the optimal sintering process time, the speed of the sintering belt is determined, and through the optimal value of the gas valocity, the pressure in the vacuum chambers is determined, according to the Ergun equation (2.6). The simulation results of the sintering point control system for the first sample are shown on Figure 5.2. The structure of the control system looks as follows: from the beginning of the process, the system accumulates 15 values (for this example, up to 7.5 minutes of the sintering process), on the basis of which a grey model is created. The grey model predicts the temperature at the end of the sintering belt for given initial values of speed and pressure. The difference between the predicted and target value starts the prediction process. Results of prediction optimization of the 1st sample: the speed values vary from 3.5 m/min to 4.5 m/min and the pressure in the vacuum chambers from 800 mm Hg up to 760 mm Hg. Therefore, the sintering point can be reached in 17.5 minutes instead of 22 minutes, when the gas velocity changes from 0.48 m/s to 0.52 m/s.

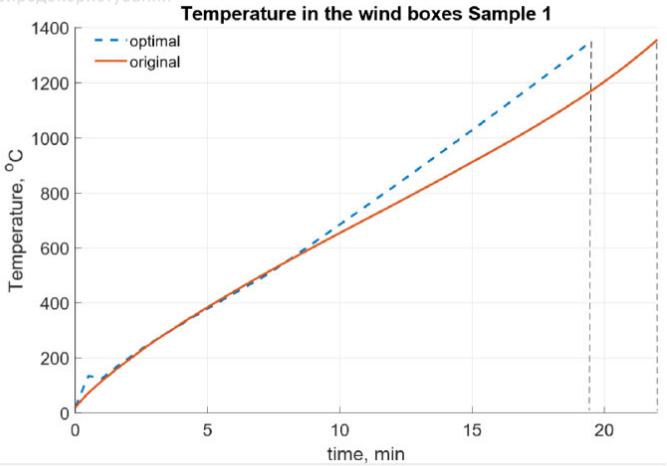

Fig. 5.2. Results of modeling the management structure for the 1st sample

Conclusion

This paper describes the methodology and basic algorithms for modeling the agglomeration processes, starting from the beginning of the charge into the sinter machine and ending with obtaining a suitable sinter. The obtained curves of the developed mathematical model of temperature in the vacuum chambers served as the basis for testing the prediction model based on the use of the theory of grey systems and the "swarm of particles" optimization algorithm. On the basis of the developed mathematical model, there is created a sintering point prediction system, which is the basis for determining the quality of the sinter. The general structure of the sinter machine control system based on a dynamic predictive model is also proposed.

The practical significance of the developed mathematical model based on physical and chemical transformations is as follows:

- in the study of the agglomeration process: changing the composition, parametric analysis and solving optimization problems, performing mathematical experiments to improve the final product;
- the mathematical model can be used as a training platform (simulator) for agglomeration processes and the use of physical laws of heat transfer in porous materials.

The practical significance of the developed predictive model based on the theory of grey systems is as follows:

- prediction of the value of the sintering point of the sinter and the synthesis of the control action based on the prediction;

- the algorithm for creating a mathematical prediction model can be used for any process that has the character of a “grey exponential law”.

The paper is written within the framework of the project entitled «Development and testing of intelligent algorithms for optimal control of the technological process of yellow phosphorus purification in the conditions of the NDFP, IRN AP08856867.

References

1. Permanent Technological Regulation No. 3 for the production of phosphorite agglomerate for the production of yellow phosphorus. // ZHF "Kazphosphate" LLP (NDFP). - 2010. - 115 p.

2. **D. A. Aznabayev**. Improvement of the theory of solid-phase chemical reactions and intensification of the agglomeration process: il RGB OD 61:85-5/4899. Website: http://www.dslib.net/cvetn-metallurgia/sovershenstvovanie-teorii-tverdofaznyh-himicheskih-reakcij-i-intensifikacija.html.

3. **L.J. Gibson, M.F. Ashby**. Thermal, electrical and acoustic properties of foams. In Cellular Solids: Structure and Properties, 2nd ed. // Cambridge University Press: Cambridge, UK. – 1997. – P. 283-308.

4. **J. Vu.** Modelling of Convective Heat Transfer in Porous Media. // Electronic Thesis and Dissertation Repository. 4852. – 2017. Сайт: https://ir.lib.uwo.ca/etd/4852.

5. **S. Majumder, P. V. Natekar, V. Runkana**. Virtual indurator: A tool for simulation of induration of wet iron ore pellets on a moving grate. // Computers and Chemical Engineering. – 2009. – №33. – P. 1141–1152.

6. Comsol: Модуль течения в грунтах. Сайт: https://www.comsol.ru/subsurface-flow-module.

7. **Y. Kaymak, T. Hauck, M. Hillers**. Iron Ore Sintering Process Model to Study Local Permeability Control. // Excerpt from the Proceedings of the 2017 COMSOL Conference in Rotterdam. –2017. – P. 1-7.

8. **N.K. Nath, A.J. Silva, N. Chakraborti**. Dynamic process modeling of iron ore sintering. // Steel Research. – 1997. - №68. – P. 285-292.

9. **A. F. Bogatyrev, S. V. Panchenko, N. A. Skuratova**. Generalization of the dependences of the thermophysical properties of solid materials with reacting

components. Retrieved from: http://www.rusnauka.com/NIO/Phisica/bogatyrev%20a.f..doc.htm.

10.Website: https://elibrary.ru/download/elibrary_29203591_49686410.PDF

11. Chemist's Handbook Retrieved from: http://chem21.info/page/100228120038234192086243212149241006093157114160/.

12. Specific heat capacities of solids, liquids and gases (gases - at a constant pressure of 1 bar abs) + reference densities. Retrieved from: http://tehtab.ru/guide/guidephysics/guidephysicsheatandtemperature/specificheat/specificheattable/.

13. **Bobkov V. I.** Models for describing the properties of phosphate raw materials. // Uspekhi sovremennoy nauki i obrazovaniya. - 2017. - Vol. 4. - No. 4-p. 73-77.

14. Q. Feng, T. Li, X. Fan, T. Jiang. Adaptive prediction system of sintering through point based on self-organize artificial neural network. // Trans. Nonferrous Met. Soc. China. – 2000. – Vol. 10. – №6. – P. 804-807.

15. **L. Peng, Z. Ji and J. Tan**. Sintering Finish Point Intelligent Control. // Proceedings of the 2005 IEEE/ASME International Conference on Advanced Intelligent Mechatronics Monterey, California, USA . – July 24-28, 2005.

16. **S. Du, M. Wu, X. Chen, X. Lai, W. Cao**. Intelligent Coordinating control between burn-through point and mixture bunker level in an iron ore sintering process. // Journal of advanced Computational Intelligence and Intelligent Informatics. – 2017. – Vol. 21. – №1.

17. **J. Wang** et al. BTP prediction of sintering process by using multiple models. // 26th Chinese Control and Decision Conference (CCDC 2014), Changsha, China. – 2014.

18. **B. Wang, Y. Fang, J. Sheng, W. Gui, Y. Sun**. BTP Prediction Model Based on ANN and Regression Analysis. // Second International Workshop on Knowledge Discovery and Data Mining. – 2009. – P.108-111

19. **J. Wang, X. Li, Y. Li, K. Wang.** BTP prediction of sintering process by using multiple models. // 26th Chinese Control and Decision Conference (CCDC) – 2014. – P.4008-4012.

20. **M. Wu, C. Xu, Y. Du**. Intelligent optimal control for lead-zinc sintering process state // Trans. Nonferrous Met. Soc. China. – 2006. – №16. – P. 975-981.

21. **M. Wu, C. Xu, J. She, W. Cao**. Neural-network-based integrated model for predicting burn-through point in lead-zinc sintering process. // Journal of Process Control. – 2012. – Vol.22. – P. 925– 934.

22. **M. Wu, P. Duan, W. Cao, J. She and J. Xiang**. An intelligent control system based on prediction of the burn-through point for the sintering process of an iron and steel plant. // Expert Systems with Applications. – 2012. – Vol.39. – №5. – P. 5971-5981.

23. **S. Du** et al. A Fuzzy Control Strategy of Burn-Through Point Based on the Feature Extraction of Time Series Trend for Iron Ore Sintering Process. // IEEE Transactions on Industrial Informatics. – 2019. – P. 1–9.

24. **X. Chen** et al. T-S Fuzzy Logic Based Modeling and Robust Control for Burning-Through Point in Sintering Process. // IEEE Transactions on Industrial Electronics. – 2017. – №64. – P. 9378–9388.

25. **W. Cheng**. An application of adaptive genetic-neural algorithm to sinter's BTP process. // Proceedings of the Third International Conference on Machine Learning and Cybernetics, Shanghai. – August 26-29, 2004.

26. **W. Cheng**. Prediction system of burning through point (BTP) based on adaptive pattern clustering and feature map. // Proceedings of the Fifth International Conference on Machine Learning and Cybernetics, Dalian. – August 13-16, 2006.

27. **X. Shang, J. Lu, Y. Sun, J. Liu, Y. Ying.** Data-Driven Prediction of Sintering Burn-Through Point Based on Novel Genetic Programming. // Journal of iron and steel research, International. – 2010. – Vol.17. – №12. – P. 1-10.

28. **D. Wang** et al. Application Research Based on GA-FWA in Prediction of Sintering Burning Through Point. // International Conference on Computer, Communications and Mechatronics

29. **W. H. Kwon, Y. H. Kim, S. J. Lee and K. Paek**. Event-Based Modeling and Control for the Burnthrough Point in Sintering Processes. // IEEE Transactions On Control Systems Technology. – 1999. – Vol. 7. – №1. – P. 31-41.

30. **B. Kim** et al. Estimation of Burn-Through Point in the Sinter Process, 14th International Conference on Control. // Automation and Systems (ICCAS 2014). – 2014 – P. 1531-1533.

31. **J. Terpak, L. Dorcak, I. Kostial, L. Pivka**. Control of burn-through point for agglomeration belt. // Metalurgia. – 2005. – Vol.44. – №4. – P.281-284.

32. **C. Wang** and M. Wu. Hierarchical Intelligent Control System and Its Application to the Sintering Process. // IEEE Transactions On Industrial Informatics. – 2013. – Vol. 9. – №1. – P. 190-196.

33. **W. Cao** et al. A dynamic subspace model for predicting burn-through point in iron sintering process. // Information Sciences. – 2018. – P. 1-12.

34. **M. Wu, C. Wang, W. Cao, X. Lai, X**. Chen. Design and application of generalized predictive control strategy with closed-loop identification for burn-through point in sintering process. // Control Engineering Practice. – 2012. – Vol.20. – P.1065-1074.

35. **J. Shi** et al. Soft sensing of the burning through point in iron-making process. // IEEE International Conference on Cognitive Informatics & Cognitive Computing (ICCI*CC 2016), Palo Alto, CA, USA. – 2016.

36. **S. Du** et al. Intelligent Integrated Control for Burn-Through Point to Carbon Efficiency Optimization in Iron Ore Sintering Process. // IEEE Transactions on Control Systems Technology. – 2019.

37. **J. Shi, Y. Wu, L. Liao, X. Yan, J. Zeng and R. Yang**. Soft sensing of the burning through point in iron-making process. // Proceedings of 2016 IEEE 15th International Conference on Cognitive Informatics and Cognitive Computing, ICCI*CC. – 2016.

39. **J. Deng**. Introduction to grey system. // Journal of Grey System – 1989. – 1. – P. 1–24.

41. **T. Tien.** A research on the grey prediction model GM(1,n). // Applied Mathematics and Computation. – 2012. – 218. – P. 4903-4916.

40. **E. Kayacan, B. Ulutas, O. Kaynak**. Grey system theory-based models in time series prediction. // Expert Systems with Applications. – 2010. – Vol.37. – 2. – P. 1784–1789.

42. T**. L. Tien**. The indirect measurement of tensile strength of material by the grey prediction model GMC(1, n). // Measurement Science and Technology. – 2005. – 16. – P.1322–1328.

43. **T. Tien.** The indirect measurement of tensile strength for a higher temperature by the new model IGDMC(1,n). // Measurement. – 2008. – 41. – P. 662-675.

44. **T. Tien**. The indirect measurement of tensile strength by the new model FGMC (1,n). // Measurement. – 2011 – 44. – P. 1884-1897.

45. **T. Tien**. The deterministic grey dynamic model with convolution integral DGDMC(1,n). // Applied Mathematical Modelling. – 2009. – 33. – P. 3498-3510.

46. **Z. X. Wang and L. L. Pei**. An optimized grey dynamic model for forecasting the output of high-tech industry in China. // Mathematical Problems in Engineering. – 2014.

47. **J. Kennedy, R. C. Eberhart**. “Particle swarm optimization”. // In Proceedings of IEEE International Conference on Neural Networks. – 1995. – P. 1942–1948.